Accelerated Publications

Effect of ErbB2 Coexpression on the Kinetic Interactions of Epidermal Growth Factor with Its Receptor in Intact Cells†

John C. Wilkinson and James V. Staros*

Department of Biological Sciences, Vanderbilt University, Nashville, Tennessee 37235

Received October 8, 2001; Revised Manuscript Received November 18, 2001

ABSTRACT: We have extended the use of stopped-flow mixing and fluorescence anisotropy detection to investigate in real-time the effects of ErbB2 coexpression on the kinetic interactions of epidermal growth factor (EGF) with the EGF receptor. Using stable 32D-derived cell lines expressing both the EGF receptor and ErbB2, and fluorescein-labeled H22Y murine EGF (F-EGF), a series of association and dissociation experiments were performed in which the kinetic interaction of F-EGF with cells was monitored by observing time-dependent changes in fluorescence anisotropy following rapid mixing. Data were collected at various concentrations of F-EGF and multiple cell densities, using cells that express similar levels of the EGF receptor but different levels of ErbB2, and then analyzed by fitting to a two independent receptor-class model using global analysis techniques. The recovered kinetic parameters indicated that the coexpression of ErbB2 had relatively modest effects on recovered rate constants and calculated K_d values, but a significant effect on the fraction of receptors associated with the high-affinity receptor class. This effect on the fraction of high-affinity receptors depended on the relative expression of ErbB2, as higher ErbB2 expression levels correlated with a larger fraction of high-affinity receptors. Further, the increase in the fraction of high-affinity receptors due to the presence of ErbB2 occurred without any change in the total number of EGF binding sites per cell. Thus, we have identified modulation of the relative populations of high- and low-affinity classes of EGF receptors as a consequence of coexpression of ErbB2 with the EGF receptor.

The binding of EGF[1] to its receptor initiates an intracellular signal cascade leading to cellular differentiation and/or mitosis (*1*, *2*). Recent evidence has suggested that kinetic parameters that describe the dynamic interaction of EGF with its receptor may be important indicators of the strength of the signal(s) transmitted by the hormone−receptor complex (*3*). We have approached this problem by developing a stopped-flow fluorescence anisotropy[2] method for measuring the kinetic interactions of EGF with its receptor *in living cells* in real time (*4*).

The key to this method is our discovery that 32D cells, murine hematopoietic progenitor cells that are devoid of ErbB mRNAs and proteins (*5*), can survive rapid stopped-flow mixing (*4*). We established a stable monoclonal cell line (designated LE1.15) expressing the EGF receptor in this null background, and thoroughly characterized EGF−EGF receptor interactions in this system (*4*). However, cells that naturally express the EGF receptor essentially always express other members of the ErbB family, in particular ErbB2 (*6*, *7*). Further, the status of ErbB2 as the preferred heterodimerization partner of the other three ErbB receptors (*8*), and its role in the occurrence and progression of certain human cancers (*9*, *10*), warrants detailed characterization of the effects of ErbB2 coexpression on the interaction of EGF with the EGF receptor.

Several groups have measured the equilibrium binding of ^{125}I-EGF to cultured cells; however, the results of studies carried out on a variety of cell types coexpressing the EGF receptor and ErbB2 vary greatly in the number of affinity classes and the magnitude of K_d values obtained (*11*−*15*). These variations may be due to cell-specific factors that mediate the effects of ErbB2 coexpression on the interaction of EGF with the EGF receptor, technical difficulties in accurately measuring binding using radioactive ligand, or complications arising from the coexpression of ErbB3 and ErbB4 in many of the cell types studied. Kinetic experiments from a single study suggested that the effect of ErbB2 coexpression is to decrease the dissociation rate constants

† This work was supported by Grants R01 GM55056 and T32 GM08320 from the National Institutes of Health.

* Correspondence should be addressed to this author at the Department of Biological Sciences, Vanderbilt University, VU Station B 351634, Nashville, TN 37235-1634. Telephone: (615)-322-4341. Fax: (615)-343-6707. E-mail: james.v.staros@vanderbilt.edu.

[1] Abbreviations: CMF-PBS, Ca^{2+},Mg^{2+}-free phosphate-buffered saline; EGF, epidermal growth factor; mEGF, murine EGF; FACS, fluorescence-activated cell-sorting; FBS, fetal bovine serum; FITC, fluorescein 5-isothiocyanate; F-EGF, fluorescein-labeled H22Y-mEGF; PE, phycoerythrin; WCM, WEH1-3B conditioned medium; XAT, xanthine−aminopterin−thymine.

[2] Free EGF has a low anisotropy, and receptor-bound EGF has a high anisotropy. By monitoring changes in EGF anisotropy over time following rapid mixing with EGF receptor-expressing cells, rate constants governing this interaction may be determined (*4*).

10.1021/bi015839l CCC: $22.00
Published on Web 12/08/2001

by approximately 2-fold, though no association experiments were shown, and the possible effects of ErbB3 and ErbB4 coexpression in the cells used for these experiments were not addressed (*12*).

Here we describe the establishment of stable, monoclonal cell lines that express similar levels of the EGF receptor but different levels of ErbB2 and the application of these cells to kinetic analysis of EGF−receptor interactions by stopped-flow fluorescence anisotropy detection.[2] We show that while ErbB2 coexpression results in modest perturbations in the association and dissociation rate constants describing the interaction of EGF with the EGF receptor, the predominant effect of ErbB2 coexpression is to increase the fraction of high-affinity receptors at the cell surface, an effect undetectable by previous kinetic studies employing radioligand binding methods. Thus, we provide the first kinetic evidence that ErbB2 modulates the ratio of high- and low-affinity class EGF receptors at the cell surface. How this modulation of affinity states is linked to previously described effects of ErbB2 coexpression upon EGF receptor signaling, such as slowing of receptor internalization (*16*) and increased transforming potential (*17*), as well as the cellular consequences of an increased fraction of high-affinity receptors are intriguing areas for future study.

MATERIALS AND METHODS

Materials. mEGF (*18*) and F-EGF (*4*) were prepared as previously described. 528 and 9G6 antibodies, directed to the extracytoplasmic domains of the EGF receptor and ErbB2, respectively, were from Santa Cruz. FITC- and PE-conjugated antibodies were from Southern Biotechnology Associates. Xanthine, hypoxanthine, aminopterin, thymine, and mycophenolic acid as well as all buffers and salts were from Sigma. FBS and RPMI-1640 were from Gibco. G418 sulfate was from Mediatech. All other chemicals were ACS reagent grade or better. All aqueous solutions were prepared using water purified with a Mill-Q water system (Millipore).

Cell Culture. LE1.15 cells (*4*) were maintained in RPMI-1640 containing 15% FBS, 5% WCM (as a source of IL-3), and 750 μg/mL G418. L1-2l.3 and L1-2.2 cells were maintained in RPMI-1640 containing 15% FBS, 5% WCM, 750 μg/mL G418, 250 μg/mL xanthine, 15 μg/mL hypoxanthine, 10 μg/mL thymidine, 2 μg/mL aminopterin, and 25 μg/mL mycophenolic acid (XAT medium). Cells were grown at 37 °C in an atmosphere of 5% CO_2/95% air. Cell harvesting, washing, and density determination were carried out as described (*4*).

Establishment of EGFR/ErbB2 Coexpressing 32D Cells. LE1.15 cells were harvested, residual medium was removed, and cells were resuspended in CMF-PBS (137.0 mM NaCl, 8.0 mM Na_2HPO_4, 2.7 mM KCl, 1.5 mM KH_2PO_4) at a density of 3×10^7 cells/mL. Cells were then transfected with the expression vector pLTR2-ErbB2-gpt (gift of P. P. Di Fiore, European Institute of Oncology) by electroporation as described (*4*). Following transfection, cells were immediately suspended in 10 mL of RPMI-1640/15% FBS/5% WCM and allowed to recover for 18 h. For selection, cells were then harvested and suspended in XAT medium. Clonal cell lines were established by FACS as follows: transfected cells arising from selection were harvested and washed once with cold CMF-PBS. Unfixed live cells were then incubated with both the EGF receptor-specific antibody 528 and the ErbB2-specific antibody 9G6 for 20 min on ice. Following primary antibody incubation, cells were washed and then incubated for 20 min on ice with both a FITC-conjugated secondary antibody specific for 528 and a PE-conjugated secondary antibody specific for 9G6. Cells were kept on ice, and then analyzed for both EGF receptor and ErbB2 expression using a Becton-Dickinson FACStar-plus flow cytometer (run at room temperature) equipped with a Clone-Cyt integrated deposition system and Cellquest software. Once EGF receptor and ErbB2 expression was confirmed, cloning was carried out by sorting single cells of the desired FITC and PE fluorescence into wells of a 96-well microtiter plate containing XAT medium. Once putative clonal cell populations grew to sufficient density, EGF receptor and ErbB2 expression was confirmed by incubating cells with either 528 or 9G6 antibodies, followed by incubation with FITC-conjugated secondary antibodies specific for either 528 or 9G6, and then analysis by flow cytometry as described above.

Real-Time Association of F-EGF to L1-2l.3 and L1-2.2 Cells. Methods for the measurement of F-EGF association to intact cells have been described (*4*), and were repeated for both L1-2l.3 and L1-2.2 cells with the following change: the excitation light source was either as described (*4*) or a model IMA 420 air-cooled argon-ion laser (Melles Griot). Briefly, cells were harvested, washed, and resuspended in binding buffer. Cell suspensions were then mixed with F-EGF stocks to give final cell densities ranging from 1.5×10^6 to 6.0×10^6 cells/mL and final F-EGF concentrations ranging from 1.0 to 15 nM. The temperature of all instruments and reagents was maintained at 20 °C by a circulating water bath. Fluorescence intensity data were recorded and anisotropies were determined as previously described (*4*).

Real-Time Dissociation of F-EGF from L1-2l.3 and L1-2.2 Cells by Dilution. Methods for the measurement of F-EGF dissociation from intact cells have been reported and were repeated for L1-2l.3 and L1-2.2 cells as described (*4*). Briefly, cells were harvested, washed, and resuspended in binding buffer. Cell suspensions were equilibrated with F-EGF, and then these suspensions were diluted 25-, 50-, 75-, and 100-fold by hand as described (*4*). As in association experiments, the temperature of all instruments and reagents was maintained at 20 °C by a circulating water bath. Fluorescence intensity data were recorded and anisotropies were determined as previously described (*4*).

Data Analysis. To facilitate visual inspection of anisotropy data, data for all experiments were smoothed as previously described (*4*), and the smoothed association and dissociation data were then analyzed by global analysis fitting of the data using a nonlinear least-squares method (*19*) to both a one receptor-class and a two independent receptor-class model. The rate equations used for both models are described in (*4*), and the observed anisotropies were calculated from the concentrations of the individual species as previously described (*4*). The value for r_{free} was determined from control experiments to be 0.0957 ± 0.0004, and the value for r_{bound} was determined to be $\sim$0.180 (*4*). The exact value for r_{bound} was determined during nonlinear fitting. The differential rate equations for both models were solved using the method of finite difference in a subroutine incorporated into the global analysis kernal (Globals Unlimited). Error analysis of all fitting parameters for each data surface was performed using

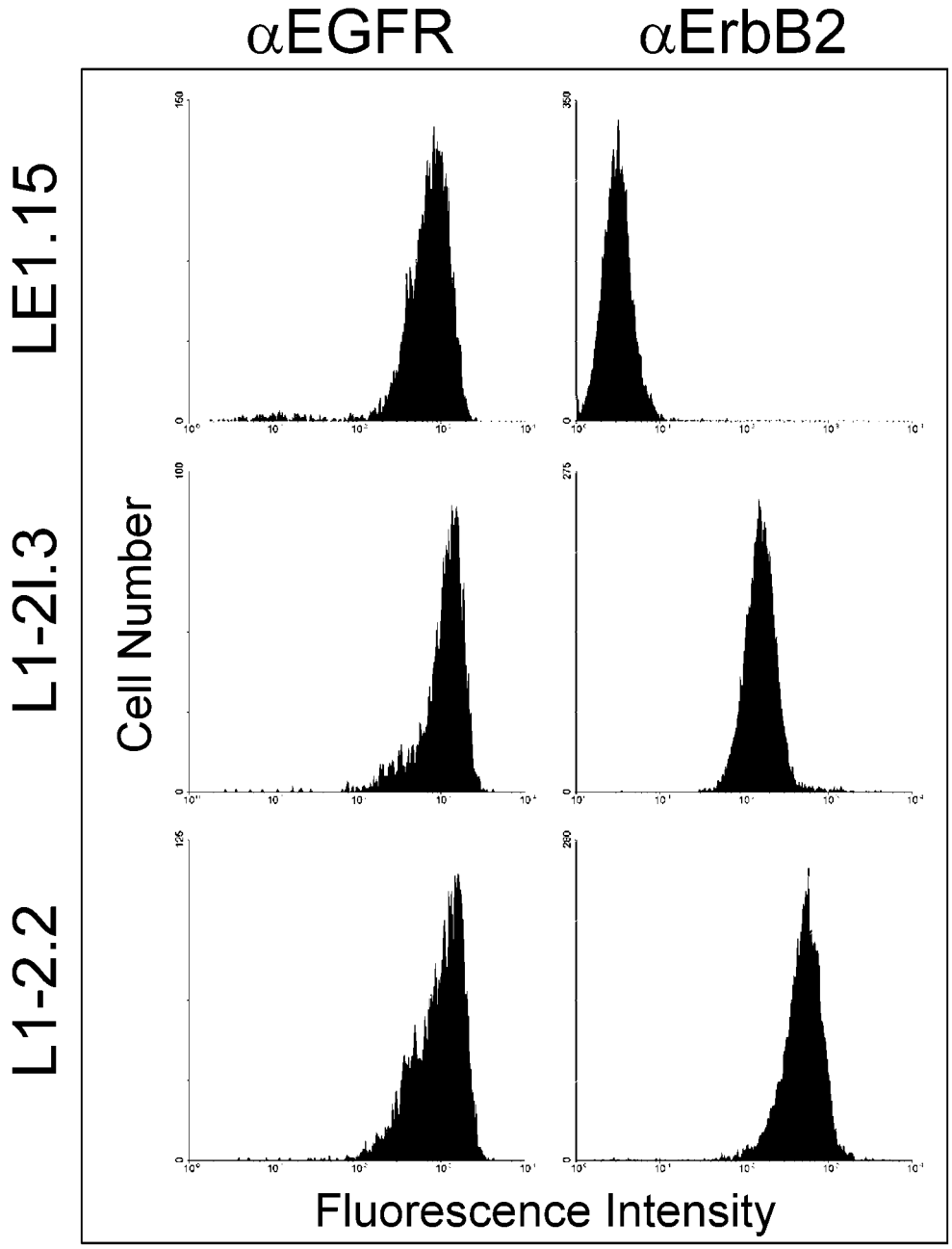

FIGURE 1: EGF receptor and ErbB2 cell surface expression in 32D transfectants. LE1.15 (top row), L1-2l.3 (middle row), and L1-2.2 cells (bottom row) were incubated with either EGF receptor-specific (left column) or ErbB2-specific (right column) antibodies followed by incubation with appropriate FITC-conjugated secondary antibodies and then analysis by flow cytometry.

the exhaustive search method as previously described (*4*, *20*, *21*).

RESULTS

Establishment of 32D Cells Coexpressing the EGF Receptor and ErbB2. We have previously described the establishment of a 32D-derived cell line, LE1.15, that stably expresses the EGF receptor for use in kinetic ligand binding studies (*4*). To determine the effects of ErbB2 coexpression on the interactions of EGF with the EGF receptor, we established stable cell lines that express both ErbB receptors by transfecting LE1.15 cells with the ErbB2 expression vector pLTR2-ErbB2-gpt (gift of P. P. Di Fiore), and isolating cell lines expressing both receptors by FACS. Several monoclonal cell lines expressing the EGF receptor and ErbB2 were obtained. Two cell lines in particular, designated L1-2l.3 and L1-2.2, showed cell surface EGF receptor expression levels similar to LE1.15 cells (Figure 1; approximately 1.0×10^6 and 9.0×10^5 EGF receptors/cell, respectively, compared to 7.5×10^5 for LE1.15 cells) while exhibiting different levels of ErbB2 cell surface expression (approximately 2.5×10^5 and 7.5×10^5 ErbB2 molecules/cell, respectively), and were used for subsequent kinetic analysis.

Real-Time Measurement of the Association of EGF to L1-2l.3 and L1-2.2 Cells. To determine the kinetic rate constants for EGF binding to L1-2l.3 and L1-2.2 cells, the anisotropy of F-EGF was measured as a function of time following stopped-flow mixing at multiple concentrations of F-EGF and various densities of cells. In separate experiments, measurements of F-EGF binding to L1-2l.3 and L1-2.2 cells were carried out at each of three final cell densities (6.0×10^6, 3.0×10^6, and 1.5×10^6 cells/mL) by mixing cell

suspensions 1:1 with F-EGF stocks to give final F-EGF concentrations ranging from 1.0 to 15 nM. This range of F-EGF corresponds to levels both above and below the estimated EGF receptor concentrations at each cell density for both cell lines (approximately 3−12 nM). Control experiments, in which cells were incubated with an excess of unlabeled mEGF prior to mixing with 2.0 nM F-EGF, showed that no nonspecific binding of F-EGF to either cell line occurred. The temperature of all instruments and reagents was maintained at 20 ± 1.0 °C, a temperature at which internalization of the EGF receptor following ligand binding is negligible (*4*). Samples of the resulting data surfaces are shown in Figure 2.

Real-Time Measurement of the Dissociation of EGF from L1-2l.3 and L1-2.2 Cells. The association experiments allow for the determination of both association and dissociation rate constants. However, under the conditions used, association dominates binding as the system approaches equilibrium, and the dissociation rate constants are therefore poorly defined. To better determine these dissociation rate constants for F-EGF bound to both L1-2l.3 and L1-2.2 cells, we measured dissociation rates by perturbation of equilibrium through dilution. In separate experiments, L1-2l.3 and L1-2.2 cells were equilibrated with F-EGF under conditions in which the large majority of F-EGF was bound (6.25×10^7 cells/mL, 100 nM F-EGF). Under these conditions, dilution of the system will cause a reequilibration resulting in the dissociation of F-EGF from the cells. Following equilibration at 20 °C, suspensions were diluted 25-, 50-, 75-, and 100-fold, and the resulting F-EGF dissociation was observed by monitoring changes in F-EGF anisotropy (Figure 3).

Global Analysis of Real-Time Data. We have previously used a two independent receptor-class model to describe the interaction of F-EGF with LE1.15 cells (*4*). To determine the effects of ErbB2 coexpression on the kinetic interaction of EGF with the EGF receptor, data surfaces that included both association (Figure 2) and dissociation (Figure 3) experiments for both L1-2l.3 and L1-2.2 cells were subjected to global analysis using the two independent receptor-class model so that recovered kinetic parameters could be directly compared to those recovered for F-EGF binding to LE1.15 cells, and the results of these analyses are shown in Table 1. For both data surfaces, we also compared the fits obtained using the two independent receptor-class model (Table 1) to fits obtained using a single receptor-class model (data not shown). The use of the two independent receptor-class model resulted in a significantly better fit than the single receptor-class model when applied to L1-2l.3 cell data surface, which was expected, but when applied to the L1-2.2 cell data surface, there was no significant difference in the fits obtained using either model. However, given that essentially all of the receptors in the L1-2.2 cell line (greater than 95%, see below) appear to exist in the high-affinity class when analyzed by the two independent receptor-class model, it is not surprising that the single class model fit the L1-2.2 cell data surface equally well.

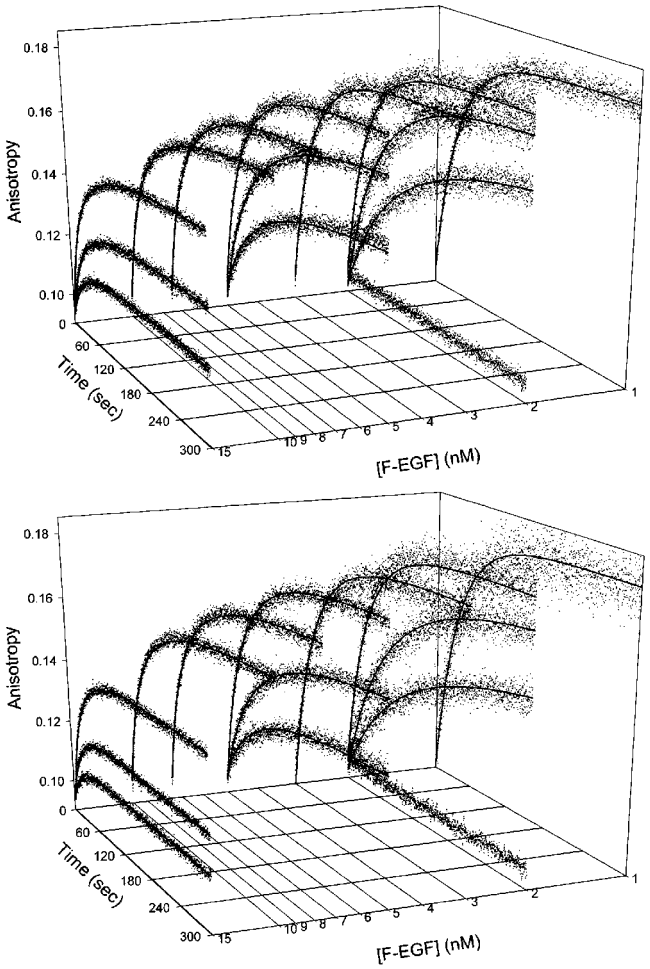

FIGURE 2: Real-time association of F-EGF to L1-2l.3 and L1-2.2 cells. L1-2l.3 cells (upper panel) and L1-2.2 cells (lower panel) were mixed with F-EGF to the following final cell densities and F-EGF concentrations: 6.0×10^6 cells/mL = 1.0, 1.5, 2.0, 3.0, 5.0, 7.5, 10.0, and 15.0 nM F-EGF; 3.0×10^6 cells/mL = 2.0, 5.0, 10.0, and 15.0 nM F-EGF; 1.5×10^6 cells/mL = 2.0, 5.0, 10.0, and 15.0 nM F-EGF. At each cell density and concentration, a total of 10 consecutive mixing experiments were performed, and the data from each mix were added together to yield the final data set. Each panel shows the anisotropy vs time for 13 of the 16 plots for each cell line; for clarity, the 1.5 nM curves at 6.0×10^6 cells/mL and the 10.0 nM curves at both 3.0×10^6 cells/mL and 1.5×10^6 cells/mL are omitted. At the 2.0 nM concentration, a representative control experiment is shown in which each cell line (6.0×10^6 cells/mL final density) was preincubated with a 50-fold excess of mEGF prior to mixing with F-EGF. The data set for each cell density and concentration consisted of 7929 data points of which every fifth point is plotted. The fit lines in each panel represent the results of fitting a combined data surface (158 444 points total) including all 16 plots from each of these experiments, as well as the plots from the corresponding dilution dissociation experiments (Figure 3), to the two independent receptor-class model (*4*). The parameter values recovered from this analysis are shown in Table 1.

DISCUSSION

We have established cells that stably express both the EGF receptor and ErbB2 in the absence of other ErbB proteins for the purpose of determining the effects of ErbB2 coexpression on the kinetic interactions of EGF with the EGF receptor. By using stopped-flow mixing coupled with fluorescence anisotropy detection, we have observed EGF association to and dissociation from cells that express similar levels of the EGF receptor but two different levels of ErbB2. Through global analysis of kinetic data surfaces collected using both cell lines, fit to a two independent receptor-class model, we have determined the changes in the kinetic interaction of EGF with the EGF receptor that occur as a result of ErbB2 coexpression.

Table 1: Recovered Parameters from Global Analysis of Association/Dissociation Data Surfaces Using the Two Independent Receptor-Class Model

parameter	LE1.15 (−SD, +SD)[a,b]	L1-2l.3 (−SD, +SD)[b]	L1-2.2 (−SD, +SD)[b]
k_{on1} ($\times 10^6$ M^{-1} s^{-1})	8.6 (5.60, 12.7)	1.6 (1.48, 1.75)	3.1 (3.06, 3.19)
k_{on2} ($\times 10^6$ M^{-1} s^{-1})	2.4 (2.01, 2.54)	3.4 (3.18, 3.78)	6.0 (3.40, 16.3)
k_{off1} ($\times 10^{-2}$ s^{-1})	0.17 (UD,[c] 0.36)	0.009 (UD,[c] 0.042)	0.09 (0.067, 0.098)
k_{off2} ($\times 10^{-2}$ s^{-1})	0.21 (0.164, 0.236)	0.29 (0.240, 0.341)	1.2 (1.00, 1.30)
K_{d1}(calcd)[d] (nM)	0.20 (UD,[c] 0.28)	0.056 (UD,[c] 0.24)	0.27 (0.22, 0.31)
K_{d2}(calcd)[d] (nM)	0.88 (0.82, 0.93)	0.86 (0.75, 0.90)	2.1 (0.79, 2.9)
% R_1[e]	12.6 (7.5, 33.0)	49.6 (42.8, 58.7)	96.6 (92.7, 98.0)
relative binding sites/cell[f]	1.00 (0.99, 1.02)	1.25 (1.23, 1.26)	1.16 (1.14, 1.19)

[a] Values as reported in Wilkinson et al., 2001 (*4*). [b] Values for each parameter were determined from analysis of a single association/dissociation data surface collected for each cell line. A total of 2−3 data surfaces were collected per cell line, and recovered parameters from the analysis of each data surface showed no significant change between replicates. Numbers in parentheses represent recovered values ± one standard deviation. [c] Lower limit undefined. [d] The K_d values were calculated such that $K_{d1} = k_{off1}/k_{on1}$ and $K_{d2} = k_{off2}/k_{on2}$. The standard deviations were calculated from the bounds of the individual rate constants, assuming the worst case. [e] Fraction of total receptors associated with k_{on1} and k_{off1}, with the remaining fraction of receptors associated with k_{on2} and k_{off2}. [f] Determined by normalizing the recovered value for receptor concentration to the value recovered for LE1.15 cells.

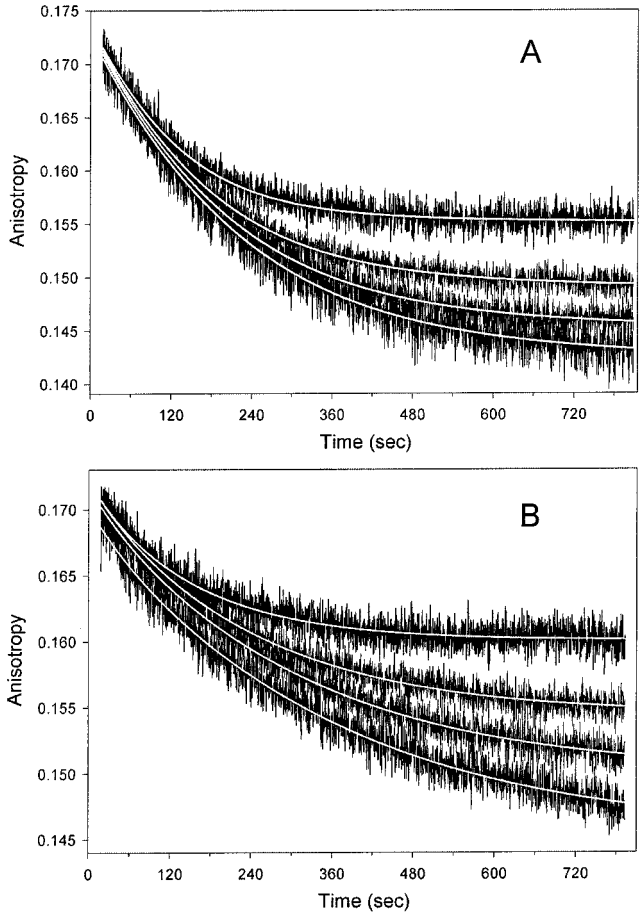

FIGURE 3: Dilution dissociation of F-EGF from L1-2l.3 and L1-2.2 cells. L1-2l.3 cells (panel A) and L1-2.2 cells (panel B) were equilibrated with F-EGF to give a final cell density of 6.25×10^7 cells/mL and a final F-EGF concentration of 100 nM. These suspensions were then mixed with SFB to give final dilutions of 25-fold (top curve), 50-fold (upper middle curve), 75-fold (lower middle curve), and 100-fold (bottom curve). At each dilution, 12−15 mixing experiments were performed, and the data from each mix were added together for the final data set. Shown are anisotropy vs time plots for each dilution. For each plot, all data points (7895 total) are shown, and sequential data points are connected by a line to present a clear separation of the data from each dilution. The fit lines represent the results of fitting a combined data surface (158 444 points total) including all 4 plots from each of these experiments, as well as the corresponding plots from the association experiment (Figure 2), to the two independent receptor-class model (*4*). The parameter values recovered from this analysis are shown in Table 1.

Inspection of the recovered parameters in Table 1 shows that, in general, the changes in rate constants for both association to and dissociation from each receptor class due to the coexpression of ErbB2 are modest, especially when the precision of the values determined, as represented by the standard deviations shown, is considered. The association rate constants are the best defined of all parameters and vary up to 5-fold, as is the case for k_{on1} (comparing LE1.15 to L1-2l.3 cells). Interestingly, k_{on1} represents the fast association rate constant for LE1.15 cells and the slow association rate constant for L1-2l.3 and L1-2.2 cells, and this "inversion" in the assignment of k_{on1} and k_{on2} to slow vs fast association states (see below) increases the variation in association rate constants recovered. The largest perturbations in recovered rate constants due to the presence of ErbB2 are observed in the dissociation rate constants for the high-affinity class (k_{off1}), consistent with a previous study (*12*). These rate constants are from 2- to 20-fold slower (L1-2.2 and L1-2l.3 cells, respectively) than observed for LE1.15 cells, though the 20-fold decrease observed for L1-2l.3 cells is based on a rate constant that, while reproducible in independent experiments, is statistically not well determined (Table 1). Of the rate constants recovered, those describing the low-affinity receptor class (k_{on2} and k_{off2}) appear to correlate with the relative level of ErbB2 coexpression, whereas those describing the high-affinity class (k_{on1} and k_{off1}) do not, and the observed changes in both the association and dissociation rate constants are reflected in modest changes for the calculated K_d values for both affinity classes.

In fitting both L1-2l.3 and L1-2.2 cell data surfaces to the two independent receptor-class model, we made no assumptions about the combination of rate constants required to describe each affinity class. We did not, for example, constrain the high-affinity class, i.e., K_{d1}, to the "slow" dissociation and "fast" association rate constants. The rate constants describing each receptor class were determined independently, and combined to calculate K_d's on the basis of a rigorous error analysis. As a result, the high-affinity receptor class for both L1-2l.3 and L1-2.2 cells was best described by the slow dissociation/slow association rate constants, which is in contrast to LE1.15 cells, for which the high-affinity receptor class is described by the slow dissociation/fast association rate constants. Any biological basis for this change in the assignment of rate constants

describing the high-affinity class is unclear, but based on rigorous error analysis, a two receptor-class model applied to both L1-2l.3 and L1-2.2 cell data surfaces in which the high-affinity receptor class is constrained to the slow dissociation/fast association rate constants (the combination that best described LE1.15 cell data) can be rejected with a confidence level greater than 95%.

More striking than the moderate changes observed in both the rate constants and the calculated equilibrium constants is the effect ErbB2 coexpression has on the fraction of receptors associated with the high-affinity class. This fraction increases as the relative expression of ErbB2 increases, such that in cells that express approximately equivalent levels of the EGF receptor and ErbB2 (L1-2.2 cells), essentially all (greater than 95%) of the receptors exist in the high-affinity state. Further, this change in the fraction of high-affinity receptors occurs without alteration of the total number of EGF binding sites per cell, as variations in the number of EGF binding sites in each cell line (Table 1) correlate with differences in the total amount of EGF receptor expressed (as determined by antibody staining and flow cytometry; Figure 1), not with the coexpression of ErbB2.

The only previous study of which we are aware that has reported experiments investigating the kinetic effects of ErbB2 on the interaction of EGF with the EGF receptor suggested that ErbB2 coexpression decreases the dissociation rate constant by approximately 2-fold, though no attempts to calculate the errors in the fits were presented (*12*). While no association experiments were shown, it was further reported that no change in the association rate constants was observed (*12*). The decrease in the dissociation rate constant observed due to the coexpression of ErbB2 was based on analysis of dissociation data in terms of a single rate constant, an approach that was warranted given that the data density was not sufficient to accurately describe the presence of more than a single receptor class. However, since equilibrium experiments performed in the same study clearly showed the presence of two receptor classes in the cells examined, interpretation of the 2-fold decrease in the dissociation rate constants reported is difficult. The reported kinetic experiments did not rule out the possibility that, rather than changing the dissociation rate constant, ErbB2 coexpression simply shifted the ratio of high- and low-affinity receptor classes present, an effect that would appear as a change in dissociation rate constants when the data were analyzed in terms of a single receptor class. Furthermore, the possible effects of ErbB3 and ErbB4 coexpression in the cells used for these experiments were not addressed (*12*). While our results generally agree with this study in terms of the effect ErbB2 coexpression has upon the recovered dissociation rate constants, our data density and subsequent rigorous analysis provide sensitivity to changes in the fraction of high-affinity receptors, an effect that was undetectable with previous kinetic methods. Additionally and unlike the previous study, we observed changes in the association rate constants due to the coexpression of ErbB2, though these changes appear to be compensatory with the changes observed in dissociation rate constants, since the calculated K_d values based on these rate constants are generally similar to those calculated for cells that do not express ErbB2.

Previous studies in which equilibrium binding of ^{125}I-EGF was analyzed by the Scatchard transform have suggested that the presence of ErbB2 is required for the high-affinity state of the receptor (*12*), creates a tiny proportion of super-high-affinity states (*11*), or has effects that are "not remarkable" (*13*). The first of these, that ErbB2 is required for the high-affinity state, has been disproved by our previous data showing that the EGF receptor expressed in the absence of any other ErbB family members exhibits two affinity states in intact cells (*4, 22*), and by the complementary observation of Burgess, Nice, and co-workers that the expressed extracytoplasmic domain of the EGF receptor exhibits two affinity states in vitro (*23*). Further, the radioligand binding approach as it has been applied to the question of ErbB2 effects is limited, because the high-affinity class is often defined by a small number ($\leq$5) of data points, and because in the naturally occurring cell lines that have been used, ErbB3 and/or ErbB4 are often coexpressed, potentially confounding the specific effects attributable to ErbB2. Thus, while the theme of associating the presence of ErbB2 with high-affinity binding of EGF has been put forward previously, our specific finding, that ErbB2 modulates the proportion of EGF receptors in the high-affinity state, is an entirely new one.

The two independent receptor-class model applied here, while admittedly wanting in its inability to correlate with the physiology of the system (*4, 22*), has been widely applied (*4, 21*−*25*), and its application in this study allows the most direct comparison with the body of published work on this system. Indeed, the kinetic and thermodynamic parameters of the high- and low-affinity states depend on the model applied. Despite intense efforts, the exact nature of the high- and low-affinity states of the EGF receptor remains unclear. Given the importance attributed to the high-affinity receptor class in signaling (*26, 27*), a thorough understanding of the factors giving rise to the high-affinity receptor class is critical. Receptor phosphorylation states (*28*−*30*), association with the cytoskeletal network (*31, 32*), and ligand-independent dimerization (*33, 34*) have all been implicated in mediating high-affinity EGF binding to the EGF receptor, and the high-affinity receptor class may arise from a combination of some or all of these factors, though this would imply interconvertable, rather than independent, receptor states. As mentioned above, the high-affinity class of the receptor has also been attributed to heterodimerization with ErbB2 (*11*−*13*); however, the high-affinity state appears to be an intrinsic property of the EGF receptor alone, since it has been observed that cells that express the EGF receptor in the absence of other ErbB family members (*4, 22*) and expressed extracytoplasmic domains of the EGF receptor in vitro (*23*) manifest high- and low-affinity receptor states. In this study, we show that the effect of ErbB2 coexpression on the interaction of EGF with the EGF receptor is to increase the fraction of high-affinity receptors. Since the high-affinity class of the EGF receptor has been shown to be both necessary and sufficient for EGF-mediated signaling through the EGF receptor (*26, 27*), our observation that ErbB2 coexpression alters the ratio of high- and low-affinity class EGF receptors is likely of physiological significance. The mechanism by which ErbB2 coexpression mediates the fraction of high-affinity EGF receptors is unclear, but may be the result of specific determinants present in ErbB2, such as specific regions in the extracytoplasmic or kinase domains. Understanding the specific molecular determinants of ErbB2

that mediate the increase in the fraction of high-affinity EGF receptors and also the cellular consequences of this increase in terms of responsiveness to EGF and subsequent mitogenic progression remain interesting areas for further study.

ACKNOWLEDGMENT

We thank Dr. J. Beechem for guidance in instrument design and global analysis matters, Dr. P. Di Fiore for providing the pLTR2-ErbB2-gpt expression vector, Dr. R. Stein and Dr. J. Ewald for critical discussions, and Dr. A. Beth for critical reading of the manuscript.

REFERENCES

1. Daly, R. J. (1999) *Growth Factors 16*, 255−263.
2. Hackel, P. O., Zwick, E., Prenzel, N., and Ullrich, A. (1999) *Curr. Opin. Cell Biol. 11*, 184−189.
3. Lenferink, A. E. G., van Zoelen, E. J. J., van Vugt, M. J. H., Grothe, S., van Rotterdam, W., van de Poll, M. L. M., and O'Connor-McCourt, M. D. (2000) *J. Biol. Chem. 275*, 26748−26753.
4. Wilkinson, J. C., Stein, R. A., Guyer, C. A., Beechem, J. M., and Staros, J. V. (2001) *Biochemistry 40*, 10230−10242.
5. Wang, L. M., Kuo, A., Alimandi, M., Veri, M. C., Lee, C. C., Kapoor, V., Ellmore, N., Chen, X. H., and Pierce, J. H. (1998) *Proc. Natl. Acad. Sci. U.S.A. 95*, 6809−6814.
6. Harari, D., and Yarden, Y. (2000) *Oncogene 19*, 6102−6114.
7. Olayioye, M. A., Neve, R. M., Lane, H. A., and Hynes, N. E. (2000) *EMBO J. 19*, 3159−3167.
8. Graus-Porta, D., Beerli, R. R., Daly, J. M., and Hynes, N. E. (1997) *EMBO J. 16*, 1647−1655.
9. Hynes, N. E., and Stern, D. F. (1994) *Biochim. Biophys. Acta 1198*, 165−184.
10. Klapper, L. N., Kirschbaum, M. H., Sela, M., and Yarden, Y. (2000) *Adv. Cancer Res. 77*, 25−79.
11. Wada, T., Qian, X. L., and Greene, M. I. (1990) *Cell 61*, 1339−1347.
12. Karunagaran, D., Tzahar, E., Beerli, R. R., Chen, X., Graus-Porta, D., Ratzkin, B. J., Seger, R., Hynes, N. E., and Yarden, Y. (1996) *EMBO J. 15*, 254−264.
13. Pinkas-Kramarski, R., Soussan, L., Waterman, H., Levkowitz, G., Alroy, I., Klapper, L., Lavi, S., Seger, R., Ratzkin, B. J., Sela, M., and Yarden, Y. (1996) *EMBO J. 15*, 2452−2467.
14. Worthylake, R., Opresko, L. K., and Wiley, H. S. (1999) *J. Biol. Chem. 274*, 8865−8874.
15. Johannessen, L. E., Haugen, K. E., Ostvold, A. C., Stang, E., and Madshus, I. H. (2001) *Biochem. J. 356*, 87−96.
16. Wang, Z., Zhang, L., Yeung, T. K., and Chen, X. (1999) *Mol. Biol. Cell 10*, 1621−1636.
17. Kokai, Y., Myers, J. N., Wada, T., Brown, V. I., LeVea, C. M., Davis, J. G., Dobashi, K., and Greene, M. I. (1989) *Cell 58*, 287−292.
18. Savage, C. R., Jr., Inagami, T., and Cohen, S. (1972) *J. Biol. Chem. 247*, 7612−7621.
19. Beechem, J. M. (1992) *Methods Enzymol. 210*, 37−54.
20. Johnson, M. L., and Frasier, S. G. (1985) *Methods Enzymol. 117*, 301−342.
21. Rousseau, D. L., Jr., Staros, J. V., and Beechem, J. M. (1995) *Biochemistry 34*, 14508−14518.
22. Stein, R. A., Wilkinson, J. C., Guyer, C. A., and Staros, J. V. (2001) *Biochemistry 40*, 6142−6154.
23. Domagala, T., Konstantopoulos, N., Smyth, F., Jorissen, R. N., Fabri, L., Geleick, D., Lax, I., Schlessinger, J., Sawyer, W., Howlett, G. J., Burgess, A. W., and Nice, E. C. (2000) *Growth Factors 18*, 11−29.
24. Gill, G. N., Bertics, P. J., and Santon, J. B. (1987) *Mol. Cell. Endocrinol. 51*, 169−186.
25. Mayo, K. H., Nunez, M., Burke, C., Starbuck, C., Lauffenburger, D., and Savage, C. R., Jr. (1989) *J. Biol. Chem. 264*, 17838−17844.
26. Bellot, F., Moolenaar, W., Kris, R., Mirakhur, B., Verlaan, I., Ullrich, A., Schlessinger, J., and Felder, S. (1990) *J. Cell Biol. 110*, 491−502.
27. Defize, L. H., Boonstra, J., Meisenhelder, J., Kruijer, W., Tertoolen, L. G., Tilly, B. C., Hunter, T., van Bergen en Henegouwen, P. M., Moolenaar, W. H., and de Laat, S. W. (1989) *J. Cell Biol. 109*, 2495−2507.
28. Countaway, J. L., McQuilkin, P., Girones, N., and Davis, R. J. (1990) *J. Biol. Chem. 265*, 3407−3416.
29. Gray, G. M., and Macara, I. G. (1988) *J. Biol. Chem. 263*, 10714−10719.
30. Friedman, B., Fujiki, H., and Rosner, M. R. (1990) *Cancer Res. 50*, 533−538.
31. Wiegant, F. A., Blok, F. J., Defize, L. H., Linnemans, W. A., Verkley, A. J., and Boonstra, J. (1986) *J. Cell Biol. 103*, 87−94.
32. Roy, L. M., Gittinger, C. K., and Landreth, G. E. (1989) *J. Cell. Physiol. 140*, 295−304.
33. Sorokin, A., Lemmon, M. A., Ullrich, A., and Schlessinger, J. (1994) *J. Biol. Chem. 269*, 9752−9759.
34. Gadella, T. W., Jr., and Jovin, T. M. (1995) *J. Cell Biol. 129*, 1543−1558.

BI015839L